Available online at www.sciencedirect.com
ScienceDirect
Trans. Nonferrous Met. Soc. China 34(2024) 2658−2670
Transactions of Nonferrous Metals Society of China
www.tnmsc.cn

Flotation separation of brucite and calcite in dodecylamine system enhanced by regulator potassium dihydrogen phosphate

Xiu-feng GONG[1], Jin YAO[1], Bin YANG[2], Wan-zhong YIN[1], Yu-lian WANG[3], Ya-feng FU[4]

1. School of Resources and Civil Engineering, Northeastern University, Shenyang 110819, China;
2. School of Chemical Engineering, China University of Mining and Technology, Xuzhou 221163, China;
3. School of Materials Science and Engineering, Shenyang Ligong University, Shenyang 110159, China;
4. Ansteel Beijing Research Institute Co., Ltd., Beijing 102200, China

Received 10 June 2023; accepted 10 November 2023

Abstract: To achieve efficient flotation separation of brucite and calcite, flotation separation experiments were conducted on two minerals using dodecylamine (DDA) as the collector and potassium dihydrogen phosphate (PDP) as the regulator. The action mechanism of DDA and PDP was explored through contact angle measurement, zeta potential detection, solution chemistry calculation, FTIR analysis, and XPS detection. The flotation results showed that when DDA dosage was 35 mg/L and PDP dosage was 40 mg/L, the maximum floating difference between brucite and calcite was 79.81%, and the selectivity separation index was 6.46. The detection analysis showed that the main dissolved component HPO_4^{2-} of PDP is selectively strongly adsorbed on the Ca site on the surface of calcite, promoting the adsorption of the main dissolved component RNH_3^+ of DDA on calcite surface, while brucite is basically not affected by PDP. Therefore, PDP is an effective regulator for the reverse flotation separation of brucite and calcite in DDA system.
Key words: brucite; calcite; selective adsorption; flotation separation

1 Introduction

In China, more than two-thirds of strategic mineral resources are at a disadvantage, but the total reserves and production of magnesium resources are both the world's largest [1]. Magnesium has many industrial uses and is mainly used in the manufacturing of magnesium alloys, as a reducing agent, and as a material for the aviation industry [2]. Among magnesium resource products, magnesium alloys are the most potential light-weight materials, exhibiting low density, high specific strength, vibration and noise reduction capacity, abundance, and environmental friendliness [3]. Brucite is a high-magnesium mineral that is a major component of magnesium resources, and its chemical formula is $Mg(OH)_2$. Brucite deposits often contain calcite, dolomite, and other carbonate minerals [4]. Calcite is a typical gangue mineral that coexists with brucite; the chemical formula of calcite is $CaCO_3$ and its specific gravity, hardness, and particle size are close to those of brucite [5]. Due to the influence of factors such as mineral density, particle size and shape on gravity beneficiation, separating calcite from brucite via gravity separation and other physical separation methods is challenging [6]. However, separation is possible using methods such as flotation that exploit the differences in the physical and chemical properties of mineral particles [7−9].

When the flotation method is used to separate calcite from brucite in a solution, one mineral floats up and the other sinks down owing to the difference

Corresponding author: Jin YAO, Tel: +86-15940036111, E-mail: yaojin@mail.neu.edu.cn
DOI: 10.1016/S1003-6326(24)66567-2

in the surface properties of the two minerals in the solution [10]. The natural floatability of oxidized minerals such as brucite and calcite is poor. Commonly oxidized ore collectors include fatty acid collectors represented by sodium oleate (NaOL) and amine collectors represented by dodecylamine (DDA) [11]. Both types of collectors can achieve the effect of mineral recovery; however, these collectors have difficulty in achieving mineral separation because they have a strong ability to collect oxidized ores but poor selectivity, which is highly evident in the case of NaOL and DDA [12]. Therefore, with respect to flotation separation, collectors must be used to achieve the separation objective under the action of a regulator; accordingly, many recent studies have focused on this aspect of flotation separation [13,14].

Recently, studies on the flotation of magnesium resources have focused on the flotation of magnesite, most of which is found in the flotation system of NaOL or DDA, to explore the effect of the regulator on the flotation separation of magnesium resources from their associated calcareous gangue minerals [15−17]. From the research results, anionic collectors such as NaOL are used for the positive flotation separation of magnesium ore resources and calcium-containing gangue minerals. Regulators can inhibit gangue minerals and reduce their floatability, thus promoting the enrichment of magnesium ore resources in mineralized bubbles [18]. However, when using cationic collectors such as DDA for reverse flotation separation, the regulator can activate gangue minerals, improve their floatability, and enrich them in mineralized bubbles, while magnesium resources are retained in the pulp for recovery [19]. Among the used adjusters, the most used adjusters include phosphoric acid and its salts, carboxylic acid and its salts, and starch and its modified sugars [14,20,21]. In addition, some recent research studies have focused on a reverse flotation system with DDA as a collector probably because DDA exhibits a good ability to collect silicate minerals from ore resources, which can be collected and removed using the reverse flotation method [19,22,23].

Currently, there are limited studies on the flotation of brucite, particularly on the reverse flotation of brucite [24]. The effectiveness of reverse flotation methods in the separation of brucite must be further explored. In this study, reverse flotation experiments were conducted on brucite and calcite using DDA as the collector and PDP as the activator. After achieving good sorting results, methods such as zeta potential measurement, contact angle measurement, solution chemical analysis, Fourier-transform infrared (FTIR) analysis, and X-ray photoelectron spectroscopy (XPS) detection were used to thoroughly analyze the internal reasons for the success in achieving the reverse flotation separation of brucite and calcite in the DDA system using PDP, providing a reference scheme for the flotation purification of brucite resources.

2 Experimental

2.1 Materials

The pure calcite and brucite minerals used in the experiment were all from the Dashiqiao area in Yingkou, Liaoning Province, China. Their chemical compositions are shown in Table 1. Figure 1 shows the X-ray diffraction (XRD) patterns of the two minerals, revealing the absence of other impurity peaks for the two minerals. The purity levels of calcite and brucite calculated based on the contents of CaO and MgO were 99.14% and 94.26%, respectively, meeting the requirements of the flotation test [25]. The bulk pure minerals in calcite and brucite were sorted, cleaned, manually broken, and screened, and ore samples with particle sizes of from 45 to 74 μm were selected for the flotation test. The samples with particle sizes less than 45 μm were ground to particle sizes less than 5 μm for determining the zeta potential and obtaining FTIR spectra.

2.2 Reagents

The reagents used in this study are shown in Table 2 and the structures of PDP (the regulator) and DDA (the collector) are shown in Fig. 2.

2.3 Microflotation test

The microflotation of brucite and calcite was conducted using an XFG−II mechanical agitation flotation machine (Jilin Exploration Machinery Factory, China). The flotation experiment was carried out as per the flotation test process shown in Fig. 3. After drying and weighing the recovered concentrates and tailings, the flotation recovery of

Table 1 Chemical compositions of pure mineral samples (wt.%)

Sample	MgO	CaO	SiO_2	Al_2O_3	TFe	Purity
Calcite	0.31	55.55	<0.10	0.22	<0.10	99.14
Brucite	65.15	0.35	3.27	0.15	0.14	94.26

Table 2 Reagent description used in test

Reagent	Application	Purity	Manufacturer
PDP	Regulator	Analytical grade	Shenyang Dongxing Reagent Factory, China
DDA	Collector	Chemically pure	Sinopharm Chemical Reagent Co., Ltd., China
HCl	pH adjustor	Analytical grade	Sinopharm Chemical Reagent Co., Ltd., China
NaOH	pH adjustor	Analytical grade	Shandong Usolf Chemical Technology Co., Ltd., China
KBr	IR diluent	Spectroscopic grade	Sinopharm Chemical Reagent Co., Ltd., China

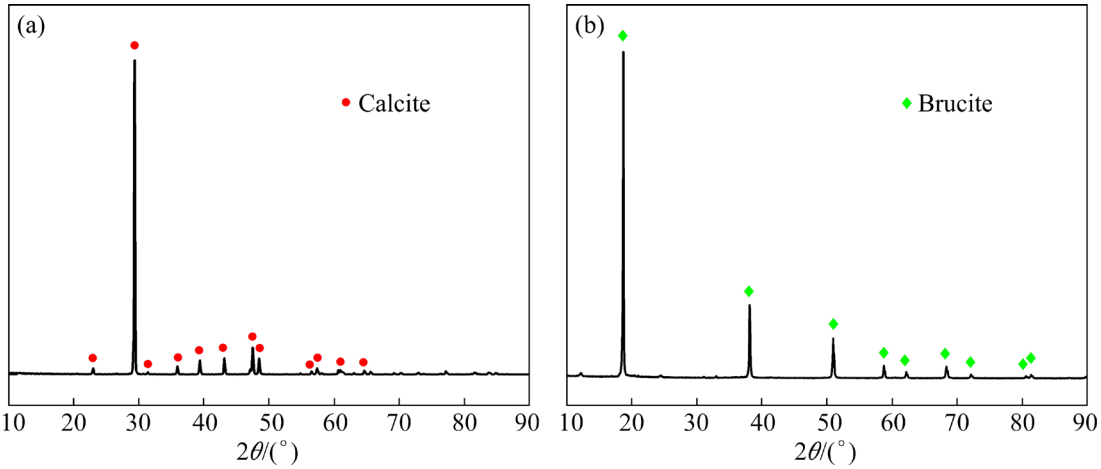

Fig. 1 XRD patterns of mineral specimens: (a) Calcite; (b) Brucite

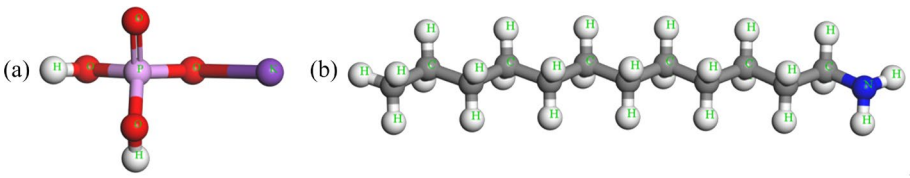

Fig. 2 Structures of PDP (a) and DDA (b)

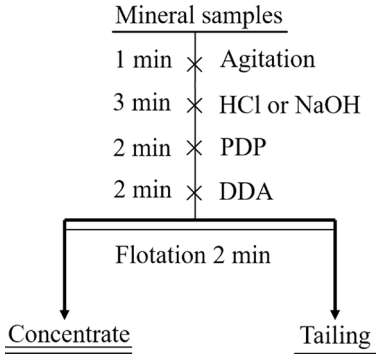

Fig. 3 Flowsheet of single-mineral and binary mixed-mineral flotation experiments

the samples was calculated based on the mass fraction and chemical analysis of the MgO and CaO in the products.

For the single-mineral and binary mixed-mineral flotation processes, mineral recovery (ε, %) is calculated using Eqs. (1) and (2), respectively:

$$\varepsilon=\frac{m_c}{m_c+m_t}\times 100\% \quad (1)$$

$$\varepsilon=\frac{\alpha m_c}{\alpha m_c+\beta m_t}\times 100\% \quad (2)$$

where m_t represents the mass of the tailings, m_c

represents the mass of the concentrate, α represents the grade of the concentrate expressed as CaO or MgO grade (%), and β represents the grade of the tailings expressed as CaO or MgO grade (%).

To quantitatively describe the flotation selectivity of calcite separated from brucite using PDP, the selectivity index (SI) shown in Eq. (3) was used as the evaluation standard [18]:

$$SI=\sqrt{\frac{\varepsilon_c^B \varepsilon_t^C}{\varepsilon_t^B \varepsilon_c^C}} \quad (3)$$

where ε represents each mineral recovery in the concentrates (expressed as the subscript c) and tailings (expressed as the subscript t) (%), and the superscripts B and C represent brucite and calcite, respectively.

2.4 Zeta potential measurement

The zeta potential measurement was performed using a ZS90−2000 potentiodynamic analyzer (Malvern Instruments Limited). In the test, 20 mg of the pure mineral sample with particle sizes less than 5 μm was placed in a 50 mL beaker and 50 mL of KCl electrolyte solution with a concentration of 1 mmol/L was added. 1 mL of the upper suspension was selected for the zeta potential measurement, the values of each group were measured thrice [26].

2.5 Contact angle measurement

The contact angle was measured using a JC2000A contact angle measuring instrument. The sample was pressed into a dense, smooth cylindrical sheet and placed on a measuring platform. Each test was repeated thrice, and the average was noted [27].

2.6 FTIR spectroscopy detection

The FTIR spectroscopy measurement was carried out using a Nicolet 380 infrared spectrometer. The samples and spectral-grade potassium bromide before and after flotation reagent action were evenly mixed at a mass ratio of 1:100 and then measured using a tablet [28].

2.7 XPS detection

The XPS measurement was performed using an ESCALAB 250 spectrometer (Thermo Scientific, USA). A neutral C 1s peak (284.80 eV) was used to calibrate all binding energies, and the Thermo Avantage software was used to analyze the test results [29].

3 Results and discussion

3.1 Flotation, contact angle and zeta potential

Based on Fig. 4, the maximum flotation recoveries of brucite and calcite are obtained when the DDA dosage is 35 mg/L and the maximum floatability difference of 58.56% is achieved between the two minerals. In addition, within the pH range of 9.5−11.5, the flotation recovery difference between calcite and brucite is the largest when the pulp pH is 10.5. Therefore, at the DDA dosage of 35 mg/L, the pulp pH of 10.5 is suitable for the flotation separation of calcite from brucite.

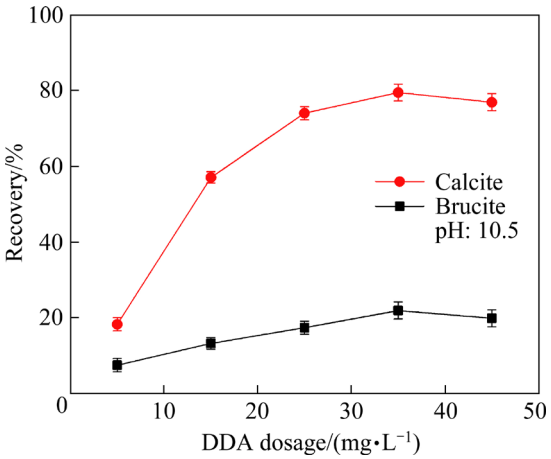

Fig. 4 Flotation recovery of brucite and calcite at different DDA dosages

As shown in Fig. 5(a), with an increase in the PDP dosage, the flotation recovery of calcite slightly fluctuates above 94%, whereas that of brucite first decreases and then increases. When the PDP dosage is 40 mg/L, the flotation recovery of brucite is 16.62% and the floatability difference between the two minerals is 79.81%. Therefore, at the DDA dosage of 35 mg/L and pH 10.5, the PDP dosage of 40 mg/L was used as the optimal dosage of the regulator for the flotation separation of calcite from brucite.

Wettability is one of the important physical and chemical characteristics of mineral surfaces and is the most intuitive indicator of mineral floatability. It depends on a highly hydrophobic particle in the bubble−particle attachment and is reflected by the size of the contact angle [30]. Mineral surface wettability (floatability) and its regulation are very

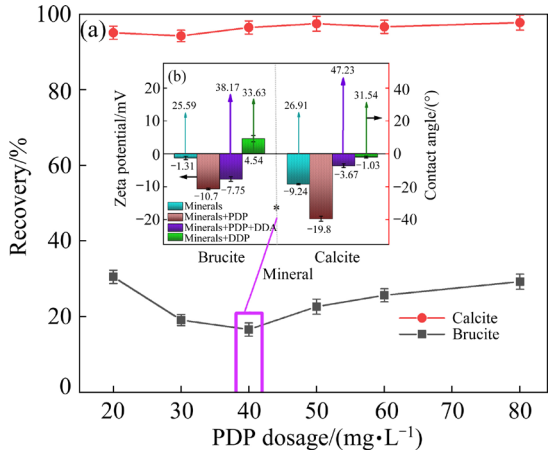

Fig. 5 Effect of PDP dosage on floatability, wettability, and charge of brucite and calcite at DDA dosage of 35 g/L and pH 10.5: (a) Flotation recovery; (b) Zeta potential and contact angle

important for realizing the flotation separation of various minerals.

In Fig. 5(b), the contact angles of pure brucite and calcite are 25.59° and 26.91°, respectively. When the collector DDA was separately added, the contact angles of both minerals increased to a certain extent, indicating that the floatability of the two minerals was enhanced to a certain extent but the increase was limited. Due to the physical adsorption of DDA on the surfaces of two minerals, the change in contact angle between the two minerals is relatively small under the action of DDA [31,32]. When PDP and DDA were added, the contact angles of the two minerals increased. The contact angle of brucite slightly increased; however, the contact angle of calcite substantially increased, reaching 47.23°, indicating that the floatability of calcite increased to a greater extent. The presence of PDP can increase the contact angles of the two minerals; however, the presence of PDP substantially affects the contact angle of calcite, considerably increasing its floatability. Moreover, this effect is not discernible in the case of brucite.

When the mineral and collector primarily rely on electrostatic attraction (physical adsorption), the adsorption of the collector on the mineral surface will primarily depend on the electrical properties of the mineral surface such as positive, negative, and absolute values of the electrical properties and differences in the electrical properties of symbiotic minerals. According to the XDLVO theory, any particle with positive charge will have a favorable interaction with a bubble [33]. Therefore, one of the important methods for investigating the mechanism of interaction between reagents and mineral surfaces and determining mineral floatability is to analyze the electrical properties of mineral surfaces and their variations.

Figure 5(b) shows that under the flotation test condition of pH 10.5, the zeta potential values of brucite and calcite are negative. The zeta potential value of brucite is −1.31 mV (close to 0), which indicates that the isoelectric point value of brucite is larger but less than 10.5. When PDP acted alone on the brucite and calcite surfaces, their zeta potentials exhibited distinct negative shifts of 9.39 and 10.56 mV, respectively, indicating that the PDP adsorption capacity of these mineral surfaces is similar. Owing to the relatively large zeta potential offset, the PDP adsorption capacity of the mineral surfaces is better.

When DDA acted alone on the brucite and calcite surfaces, their zeta potentials exhibited positive shifts of 5.85 and 8.21 mV, respectively. The offset shows that the DDA adsorption capacity of calcite is stronger than that of brucite. When PDP and DDA acted together on the brucite and calcite surfaces, the zeta potential of brucite exhibited a positive shift of 2.95 mV compared with that of PDP acting alone, and that of calcite exhibited a positive shift of 16.13 mV compared with that of PDP acting alone. This indicates that PDP adsorption is not conductive to DDA adsorption on the brucite surface. However, after PDP absorption on the calcite surface, DDA could still be adsorbed.

In addition, compared with the zeta potential offset of the two minerals in the presence of DDA alone, the zeta potential offset of brucite decreases, and that of calcite increases in the simultaneous presence of PDP and DDA. Thus, the presence of PDP can reduce the DDA adsorption capacity of the brucite surface and further enhance the DDA adsorption capacity of the calcite surface. These characteristics indicate that the presence of PDP is conducive to enhancing the flotation separation of calcite and brucite in the DDA system.

The binary mixed-mineral flotation test is a flotation effect verification test based on the single-mineral flotation test. Under the optimal flotation separation conditions determined via the single-mineral flotation test, the binary mixed-mineral flotation test of brucite (1.8 g) and calcite

(0.2 g) is helpful for verifying the separation effect of PDP on the flotation separation of the two minerals. The test results are shown in Table 3.

Table 3 shows that without PDP, the grades of MgO and CaO in the concentrate are 62.02% and 3.07%, respectively, which are slightly higher than that of the raw mixed ore, and the recovery of calcite is 39.29%, indicating that the calcite content in the concentrate is relatively high. Furthermore, an SI value of 3.10 indicates that the flotation separation of the two minerals in the DDA system exerts a certain sorting effect; however, this effect is not adequately conspicuous. When PDP is added, the grade of MgO in the concentrate is 64.44%, which is 2.42% higher than that without PDP, and the grade of CaO is 1.05%, which is 2.02% lower than that without PDP. This change reflects the effect of PDP, and the recovery of calcite in the concentrate decreases to 7.77%, which is a substantial decrease. Furthermore, after the addition of PDP, the SI value considerably increases to 6.46, further demonstrating the distinct effect of PDP on the flotation separation of calcite from brucite. These results indicate that PDP is a regulator that can realize the flotation separation of calcite from brucite.

3.2 Dissolved components

By analyzing the equilibrium of dissolution, dissociation, and association of flotation reagents in a solution, the active components of the regulator and collector can be identified and the optimal range of conditions for the interaction between flotation reagents and minerals can be determined, thus providing a theoretical basis for the selection and determination of the flotation separation conditions of minerals [11,34]. Figures 6(a) and (b) show the dissolved components of the regulator PDP and the collector DDA in the solution, respectively.

As shown in Fig. 6(a), the hydrolyzed components of PDP include H_3PO_4, $H_2PO_4^-$, HPO_4^{2-}, and PO_4^{3-}. For PDP with a concentration of 2.94×10^{-4} mol/L, HPO_4^{2-} is the dominant component in the range of $7.2 \le pH < 12.4$, and HPO_4^{2-}, PO_4^{3-} and $H_2PO_4^-$ exist at pH 10.5. The adsorption of the negatively charged components of PDP on the mineral surface is crucial to its floatability. As shown in Fig. 6(b), the critical pH of the DDA solution with a concentration of 1.89×10^{-4} mol/L is 9.74. In alkaline solutions with $pH > 9.74$, DDA primarily exists in the form of amine molecules or

Table 3 Flotation results of mixed brucite and calcite in absence and presence of PDP

Condition	Product	Yield/%	Grade/%		Recovery/%		SI
			MgO	CaO	Brucite	Calcite	
pH: 10.5; DDA: 35 mg/L	Concentrate	81.48	62.02	3.07	86.17	39.29	3.10
	Tailings	18.52	43.89	18.21	13.83	60.71	
	Feed	100.00	58.67	5.87	100.00	100.00	
pH: 10.5; DDA: 35 mg/L; PDP: 40 mg/L	Concentrate	70.84	64.44	1.05	77.85	7.77	6.46
	Tailings	29.16	44.64	17.57	22.15	92.23	
	Feed	100.00	58.67	5.87	100.00	100.00	

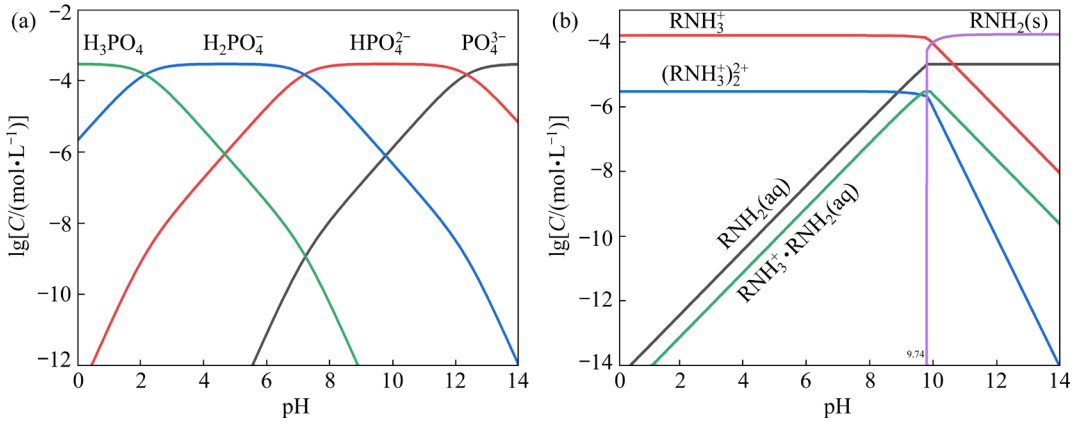

Fig. 6 lg *C*–pH curves of PDP (a) and DDA (b) in solution (*C* is concentration)

molecular ion copolymers and through RNH_3^+ and $RNH_2{\cdot}RNH_3^+$ on the mineral surface of the double layers via electrostatic adsorption on the surface of the negatively charged mineral such that the hydrophobicity of the mineral is enhanced.

3.3 FTIR spectra

Contact angle analysis results indicated that the presence of PDP can increase the hydrophobicity of the two minerals and considerably increase the floatability of calcite, demonstrating a strong activation effect on calcite. Because the activation was realized through the adsorption of the flotation reagents, the PDP and DDA adsorption characteristics on the two mineral surfaces were measured using FTIR spectroscopy; the results are shown in Figs. 7−9.

In the FTIR spectra of DDA (Fig. 7), the antisymmetric stretching vibration peaks of —NH_2, —CH_3, and —CH_2 are located at 3333.23, 2955.86, and 2921.70 cm^{-1}, respectively, and the symmetric stretching vibration peak of —CH_2 appears at 2851.62 cm^{-1}. The variable-angle vibration peaks of —NH_2 are located at 1649.58, 1568.01, and 1488.62 cm^{-1}, the —CH_3 symmetric variable-angle vibration peak is located at 1388.57 cm^{-1}, the —CH_2 twisted vibration peak is located at 1321.02 cm^{-1}, and the C—N stretching vibration peak is located at 1151.99 cm^{-1}. In addition, the N—H plane bending vibration peak is observed at 720.45 cm^{-1} [17,19,32,35]. In the FTIR spectrum of PDP, the PO—H stretching vibration peaks are observed at 2857.18, 2773.03, and 2447.76 cm^{-1}, the —PO_2 antisymmetric stretching vibration peak is observed at 1299.24 cm^{-1}, and the —PO_2 symmetric stretching vibration peak is observed at 1099.87 cm^{-1}. The P—$(OH)_2$ symmetric stretching vibration peak is observed at 908.23 cm^{-1}, while the PO_4 asymmetric variable-angle vibration peak is observed at 535.13 cm^{-1} [36,37].

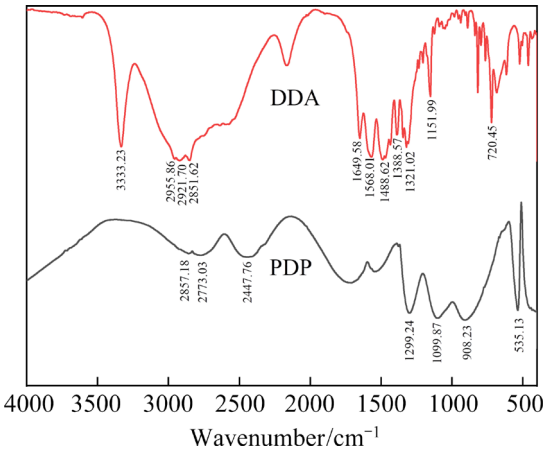

Fig. 7 FTIR spectra of flotation reagents PDP and DDA

As shown in Fig. 8, the characteristic peaks of brucite appear at 3697.46, 1483.78, 1423.63, 1075.87, and 961.31 cm^{-1}. When DDA acts alone on the brucite surface, the characteristic peaks of DDA appear at 2954.15, 2918.45, and 2851.54 cm^{-1}; the peak located at 2954.15 cm^{-1} is the CH_3 antisymmetric stretching vibration peak of DDA, and the peaks located at 2918.45 and 2851.54 cm^{-1} are the —CH_2 antisymmetric stretching vibration peak and symmetric stretching vibration peak of DDA, respectively. This observation indicates that DDA can be effectively adsorbed on the brucite surface. When PDP acts alone on the brucite surface, new peaks appear at 2820.82, 1575.83, and 552.09 cm^{-1}, indicating that PDP is adsorbed on the brucite surface. When both PDP and DDA act on the brucite surface, the PDP peaks appear only at 2817.49, 1553.90, and 567.84 cm^{-1}, indicating that the DDA adsorption capacity of the brucite surface is considerably weak in the presence of PDP.

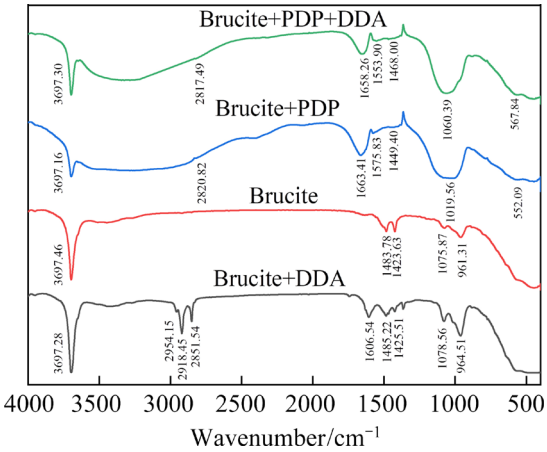

Fig. 8 FTIR spectra of brucite before and after flotation reagent action

In Fig. 9, the C—O flexural vibration peaks of calcite are observed at 712.16 and 876.41 cm^{-1}, and asymmetric vibration peak of the C—O is observed at 1421.09 cm^{-1}. When DDA acts alone on the surface of calcite, the calcite peaks appear at 3328.33, 2955.34, 2919.63, and 2851.80 cm^{-1}, indicating that DDA is adsorbed on the surface of calcite. When PDP acts alone on the surface of calcite, new peaks of calcite appear at 3542.60, 3490.63, 3162.53, 1226.48, 1133.59, 1058.58,

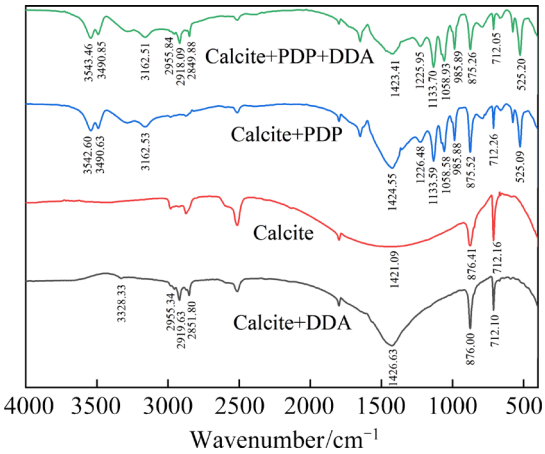

Fig. 9 FTIR spectra of calcite before and after flotation reagent action

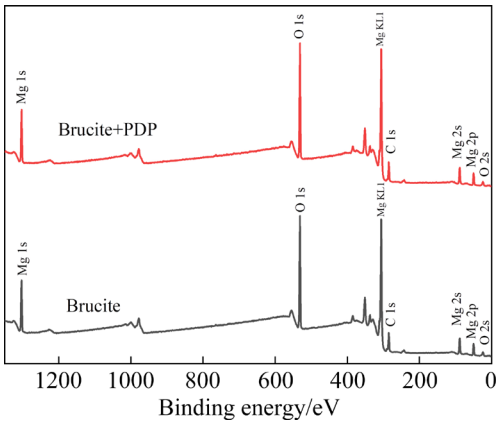

Fig. 10 Full XPS spectra of brucite before and after PDP action

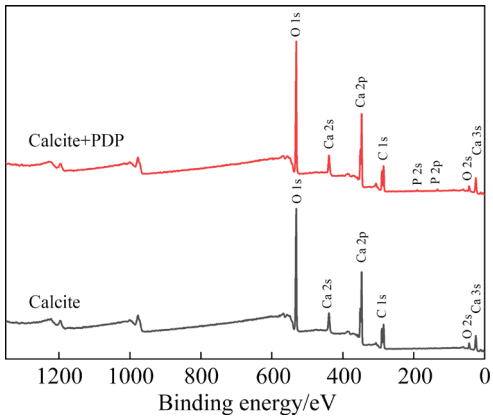

Fig. 11 Full XPS spectra of calcite before and after PDP action

985.88, and 525.09 cm^{-1}, indicating that PDP can be adsorbed on the surface of calcite. When PDP and DDA simultaneously act on the surface of calcite, the characteristic peaks of DDA appear at 2955.84, 2918.09, and 2849.88 cm^{-1} in addition to the characteristic peaks that appear when PDP acts alone on the surface of calcite, indicating that both PDP and DDA can be adsorbed on the surface of calcite. The PDP adsorption on the surface of calcite does not affect the DDA adsorption on the surface of calcite.

3.4 XPS spectra

XPS is a highly practical surface analysis method for the qualitative and quantitative analyses and structural identification of solid surfaces [38]. The adsorption mechanism of flotation reagents on the mineral surface can be understood through the characteristic changes in the element composition and element content of the mineral surface before and after flotation reagent action. Therefore, the XPS spectra of brucite and calcite as single mineral as well as binary mixed minerals treated with 40 mg/L PDP at pH 10.5 and were obtained. The full spectra of the two minerals are shown in Figs. 10 and 11.

The full XPS spectrum of brucite presented in Fig. 10 shows that three basic peaks, namely Mg 1s, O 1s, and C 1s, and several characteristic peaks, including Mg KL1, Mg 2s, Mg 2p, and O 2s, appear in the case of the surface of brucite. When PDP acts on the surface of brucite, only Mg 1s, O 1s, C 1s, Mg KL1, Mg 2s, Mg 2p and O 2s peaks are observed without any characteristic peaks of PDP, indicating that the effect of PDP on the surface of brucite is relatively weak. The adsorption effect on the surface of brucite is not discernible.

As shown in Fig. 11, three basic peaks, namely, Ca 2p, O 1s, and C 1s, and several characteristic peaks, including Ca 2s, Ca 3s, and O 2s, appear in the case of the calcite surface. When PDP acts on the surface of calcite, two characteristic peaks, namely, P 2s and P 2p, appear on the surface of calcite, indicating that the PDP adsorption on the calcite surface is relatively strong. Thus, PDP exhibits stronger adsorption capacity on the surface of calcite than that on the surface of brucite.

To understand the prominent characteristics of PDP action on the brucite and calcite surfaces, the changes in the surface element composition and content of the two minerals before and after PDP action were measured; the results are shown in Table 4.

Table 4 shows that under the action of PDP, the content of the characteristic P element that belongs

to PDP on the brucite surface increases only by 0.02 at.%, whereas that on the calcite surface increases by 1.55 at.%, which fully reflects the stronger effect of PDP on calcite than on brucite. Furthermore, with the changes in Mg and Ca, the contents of Mg and Ca are reduced by 0.31 at.% and 1.43 at.%, respectively. The interaction between PDP and calcite is stronger than that between PDP and brucite.

Table 4 Surface element compositions and contents of brucite and calcite before and after PDP action

Sample	Content/at.%				
	C 1s	O 1s	Mg 1s	Ca 2p	P 2p
Brucite	22.83	60.24	16.93		
Brucite+PDP	23.10	60.26	16.62		0.02
Shift	0.27	0.02	−0.31		0.02
Calcite	23.90	58.47		17.63	
Calcite+PDP	27.33	54.92		16.20	1.55
Shift	3.43	−3.55		−1.43	1.55

The change trends of the characteristic elements are important for understanding the influence characteristics of PDP on the mineral surface, which are reflected in the change in the molar fractions of the characteristic elements and the migration of the characteristic peaks of the characteristic elements. Figures 12 and 13 show the variation characteristics of the peaks of Mg and Ca, which are the characteristic elements of brucite and calcite, respectively.

Figure 12 shows that after PDP action, the characteristic Mg 1s peak of brucite changes from 1303.15 to 1303.14 eV, showing a decrease of 0.01 eV, thereby demonstrating the relatively weak effect of PDP on the Mg peak and its weak interaction with brucite.

Figure 13 shows that after PDP action, the Ca 2p peaks of calcite change from 346.93 and 350.47 eV to 346.87 and 350.41 eV, respectively, showing a decrease of 0.06 eV, respectively, thereby indicating the relatively strong effect of PDP on the Ca peak and its strong interaction with calcite. This

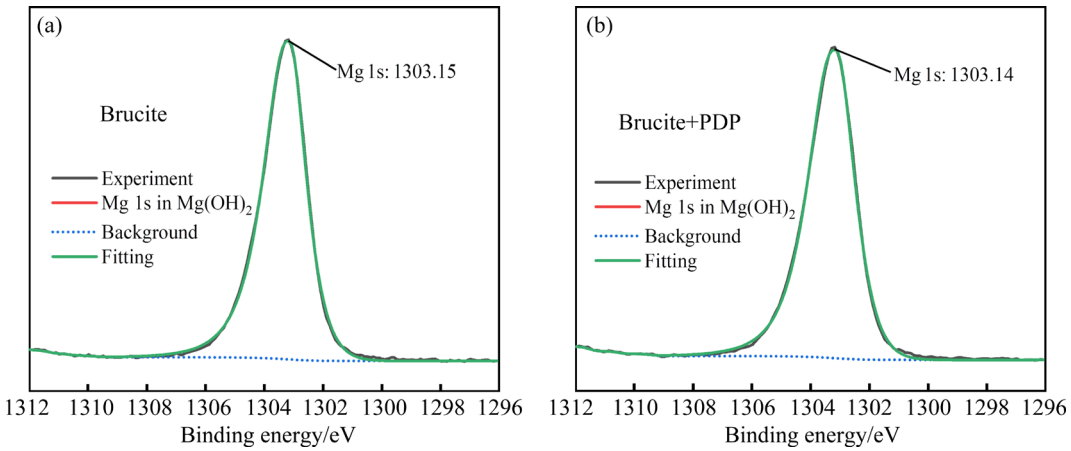

Fig. 12 XPS fitting peaks of Mg 1s on brucite surface before (a) and after (b) PDP action

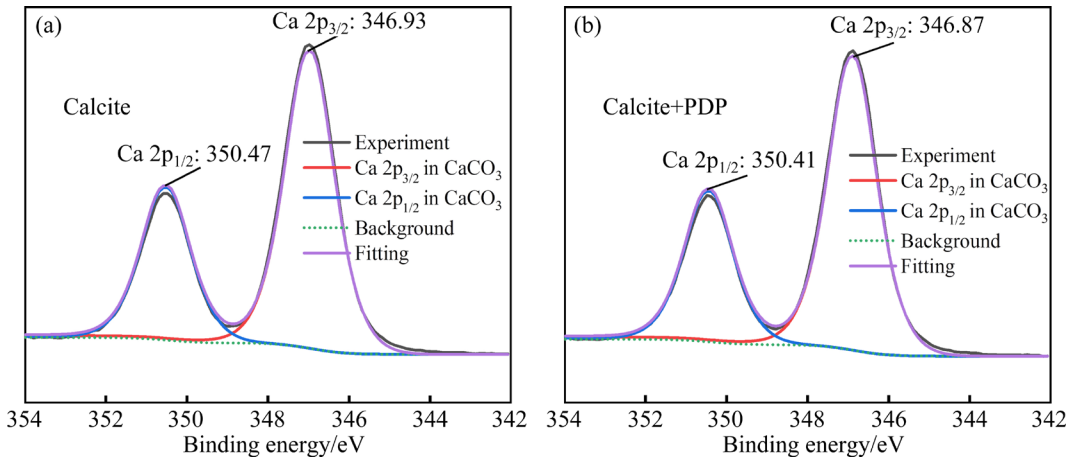

Fig. 13 XPS fitting peaks of Ca 2p on calcite surface before (a) and after (b) PDP action

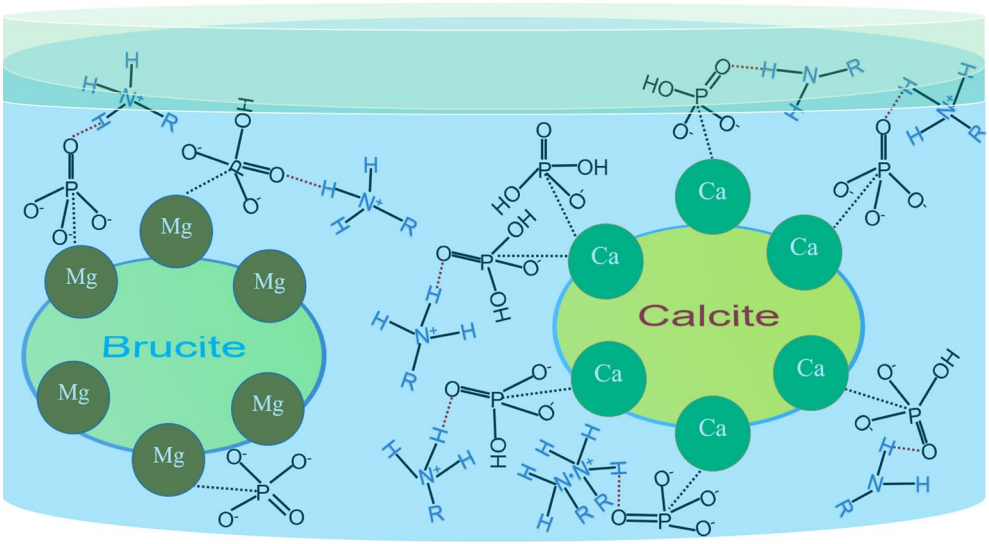

Fig. 14 Collection model of brucite and calcite by DDA after adsorption of PDP

XPS analysis shows that the strong adsorption of PDP on the surface of calcite is conducive to the ability of DDA to collect calcite, whereas the PDP adsorption on the surface of brucite is not discernible.

3.5 PDP adsorption and DDA collection

Based on previous research results on reverse flotation separation of brucite, a possible adsorption model for DDA and PDP on the surfaces of two minerals is shown in Fig. 14 [39,40]. According to XPS detection, PDP exhibits a strong affinity toward Ca sites, indicating that PDP is more likely to act on the surface of calcite with Ca sites. FTIR analysis shows that the adsorption of PDP on the surface of calcite promotes further adsorption of DDA on the surface of calcite. Solution chemical analysis shows that the dissolved components HPO_4^{2-}, PO_4^{3-}, and $H_2PO_4^-$ of PDP are negatively charged in the solution, and their adsorption on the mineral surface will cause the mineral surface to present a state of negative charge; the dissolved components of the collector DDA, i.e., RNH_3^+ and $RNH_2{\cdot}RNH_3^+$, are all positively charged in solution. Their adsorption on the mineral surface tends to be positively charged. Based on zeta potential analysis, it can be concluded that the dissolution components of PDP with negative charges can absorb more negative charges on the surface of calcite when adsorbed on the two types of mineral surfaces, which will result in calcite being in a state of strong negative charge and brucite being in a state of weak negative charge; When encountering the positively charged dissolved components of DDA, the negative charge carried by calcite will be significantly reduced, and the negative charge of brucite will slightly decrease; These results indicate that the presence of various dissolved components of PDP further promotes the adsorption of DDA on the surface of calcite, enhancing the ability of DDA to collect calcite.

4 Conclusions

(1) PDP is an effective regulator for reverse flotation separation of brucite and calcite.

(2) Negatively charged dissolved components HPO_4^{2-}, PO_4^{3-}, and $H_2PO_4^-$ of PDP strongly adsorb on calcite surface, promoting the adsorption of DDA on the surface of calcite.

(3) XPS detection shows that PDP has a strong impact on the Ca sites on calcite surface, but a weak impact on the Mg sites on brucite surface, reflecting the selectivity of PDP on calcite.

CRediT authorship contribution statement

Xiu-feng GONG: Methodology, Validation, Investigation, Writing − Original draft, Writing − Review & editing; **Jin YAO:** Supervision, Conceptualization, Project administration; **Bin YANG:** Methodology, Investigation, Writing − Review & editing; **Wan-zhong YIN:** Project administration; **Yu-lian WANG:** Visualization, Methodology; **Ya-feng FU:** Visualization.

Declaration of competing interest

The authors declare that they have no known competing financial interests or personal relationships that could have appeared to influence the work reported in this paper.

Acknowledgments

This work was financially supported by the General Program of the National Natural Science Foundation of China (Nos. 51974064, 52174239), the National Key R&D Program of China (No. 2021YFC2902400), and the Outstanding Postdoctoral Program of Jiangsu Province, China (No. 2022ZB521).

References

[1] XU Xiang-yu, LIN Yan-jun, EVANS D G, DUAN Xue. Layered intercalated functional materials based on efficient utilization of magnesium resources in China [J]. Science China: Chemistry, 2010, 53: 1461−1469. doi: 10.1007/s11426-010-4031-y.

[2] GAO Feng, NIE Zuo-ren, WANG Zhi-hong, GONG Xian-zheng, ZUO Tie-yong. Characterization and normalization factors of abiotic resource depletion for life cycle impact assessment in China [J]. Science in China Series E: Technological Sciences, 2009, 52: 215−222. doi: 10.1007/s11431-009-0028-1.

[3] GONG Xiu-feng, YAO Jin, YANG Bin, FU Ya-feng, WANG Yu-lian, YIN Wan-zhong. Selective flotation of brucite from calcite using HEDP-4Na as an inhibitor in a SDS system [J]. Journal of Industrial and Engineering Chemistry, 2023, 125: 390−401. doi: 10.1016/j.jiec.2023.05.047.

[4] XU Hui, DENG Xin-rong, Preparation and properties of superfine $Mg(OH)_2$ flame retardant [J]. Transactions of Nonferrous Metals Society of China, 2006, 16: 488−492. doi: 10.1016/s1003-6326(06)60084-8.

[5] CHEN Chen, SUN Wei, ZHU Hai-ling, LIU Run-qin. A novel green depressant for flotation separation of scheelite from calcite [J]. Transactions of Nonferrous Metals Society of China, 2021, 31: 2493−2500. doi: 10.1016/s1003−6326(21)65669-8.

[6] WANG Li, TIAN Meng-jie, KHOSO S A, HU Yue-hua, SUN Wei, GAO Zhi-yong. Improved flotation separation of apatite from calcite with benzohydroxamic acid collector [J]. Mineral Processing and Extractive Metallurgy Review, 2019, 40: 427−436. doi: 10.1080/08827508.2019.1666126.

[7] DENG Jie, LIU Cheng, YANG Si-yuan, LI Hong-qiang, LIU Yong. Flotation separation of barite from calcite using acidified water glass as the depressant [J]. Colloids and Surfaces A: Physicochemical and Engineering Aspects, 2019, 579: 123605. doi: 10.1016/j.colsurfa.2019.123605.

[8] GAO Jian-de, HU Yue-hua, SUN Wei, LIU Run-qing, GAO Zhi-yong, HAN Hai-sheng, LYU Fei, JIANG Wei. Enhanced separation of fluorite from calcite in acidic condition [J]. Minerals Engineering, 2019, 133: 103−105. doi: 10.1016/j.mineng.2019.01.013.

[9] GAO Zhi-yong, SUN Wei, HU Yue-hua. New insights into the dodecylamine adsorption on scheelite and calcite: An adsorption model [J]. Minerals Engineering, 2015, 79: 54−61. doi: 10.1016/j.mineng.2015.05.011.

[10] CHEN Wei, ZHANG Guo-fan, ZHU Yang-ge. Rheological investigations of the improved fine scheelite flotation spiked with agitation medium [J]. International Journal of Mining Science and Technology, 2022, 32: 1379−1388. doi: 10.1016/j.ijmst.2022.11.0012095-2686.

[11] YAO Jin, GONG Xiu-feng, SUN Hao-ran, HE Ruo-fan, YIN Wan-zhong. Separation of magnesite and calcite based on flotation solution chemistry [J]. Physicochemical Problems of Mineral Processing, 2022, 58: 149398. doi: 10.37190/ppmp/149398.

[12] CASES J M, VILLIERAS F, MICHOT L J, BERSILLON J L. Long chain ionic surfactants: The understanding of adsorption mechanisms from the resolution of adsorption isotherms [J]. Colloids and Surfaces A: Physicochemical and Engineering Aspects, 2002, 205: 85−99. doi: 10.1016/s0927-7757(01)01151-7.

[13] GONG Xiu-feng, YAO Jin, YANG Bin, GUO Jun, SUN Hao-ran, YIN Wan-zhong. Study on the inhibition mechanism of guar gum in the flotation separation of brucite and dolomite in the presence of SDS [J]. Journal of Molecular Liquids, 2023, 380: 121721. doi: 10.1016/j.molliq.2023.121721.

[14] LI Ming-yang, YANG Cheng, WU Zhao-yang, GAO Xiang-peng, TONG Xiong, YU Xian-kun, LONG Hong-ming. Selective depression action of taurine in flotation separation of specularite and chlorite [J]. International Journal of Mining Science and Technology, 2022, 32: 637−644. doi: 10.1016/j.ijmst.2022.03.006.

[15] ZHU Zhang-lei, FU Ya-feng, YIN Wan-zhong, SUN Hao-ran, CHEN Ke-qiang, TANG Yuan, YANG Bin. Role of surface roughness in the magnesite flotation and its mechanism [J]. Particuology, 2022, 62: 63−70. doi: 10.1016/j.partic.2021.06.007.

[16] ZHU Yang-ge, YANG Lin-feng, HU Xiao-xing, ZHANG Xing-rong, ZHENG Gui-bing. Flotation separation of quartz from magnesite using carboxymethyl cellulose as depressant [J]. Transactions of Nonferrous Metals Society of China, 2022, 32: 1623−1637. doi: 10.1016/s1003-6326(22)65898.

[17] SUN Hao-ran, YIN Wan-zhong, YAO Jin. Study of selective enhancement of surface hydrophobicity on magnesite and quartz by N, N-dimethyloctadecylamine: Separation test, adsorption mechanism, and adsorption model [J]. Applied Surface Science, 2022, 583, 152482. doi: 10.1016/j.apsusc.2022.152482.

[18] YANG Bin, YIN Wan-zhong, YAO Jin, SHENG Qiu-yue, ZHU Zhang-lei. Role of decaethoxylated stearylamine in the selective flotation of hornblende and siderite: An experimental and molecular dynamics simulation study [J]. Applied Surface Science, 2022, 571: 151177. doi: 10.1016/j.apsusc.2021.151177.

[19] SUN Hao-ran, YIN Wan-zhong, YANG Bin, HAN Fang. Simultaneous separation of quartz and dolomite from magnesite using monosodium phosphate as a regulator via reverse flotation [J]. Minerals Engineering, 2021, 172: 107185. doi: 10.1016/j.mineng.2021.107185.

[20] YAO Jin, YANG Bin, CHEN Ke-qiang, SUN Hao-ran, ZHU Zhang-lei, YIN Wan-zhong, SONG Ning-bo, SHENG Qiu-yue. Sodium tripolyphosphate as a selective depressant

for separating magnesite from dolomite and its depression mechanism [J]. Powder Technology, 2021, 382: 244−253. doi: 10.1016/j.powtec.2020.12.040.

[21] CHIMONYO W, FLETCHER B, PENG Yong-jun. Starch chemical modification for selective flotation of copper sulphide minerals from carbonaceous material: A critical review [J]. Minerals Engineering, 2020, 156: 106522. doi: 10.1016/j.mineng.2020.106522.

[22] SUN Wen-han, LIU Wen-gang, LIU Wen-bao, LI Peng-cheng, SHEN Yan-bai, DAI Shu-juan. Utilization of a novel bisphosphonic acid surfactant for reverse froth flotation of magnesite and dolomite [J]. Minerals Engineering, 2022, 185: 107668. doi: 10.1016/j.mineng. 2022.107668.

[23] WU Hong-qiang, QIU Ting-sheng, ZHAO Guan-fei, ZHU Dong-mei, LI Xiao-bo, FENG Bo. Investigations on the reverse cationic flotation separation of quartz from hematite using polyaspartic acid as depressant [J]. Applied Surface Science, 2023, 614: 156143. doi: 10.1016/j.apsusc.2022. 156143.

[24] FU Ya-feng, YIN Wan-zhong, DONG Xian-shu, SUN Chuan-yao, YANG Bin, YAO Jin, LI Hong-liang, LI Chuang, KIM H. New insights into the flotation responses of brucite and serpentine for different conditioning times: Surface dissolution behavior [J]. International Journal of Minerals, Metallurgy and Materials, 2021, 28: 1898−1907. doi: 10. 1007/s12613-020-2158-1.

[25] XU Yan-ling, HUANG Kai-hua, LI Hong-qiang, HUANG Wei, LIU Cheng, YANG Si-yuan. Adsorption mechanism of styryl phosphonate ester as collector in ilmenite flotation [J]. Transactions of Nonferrous Metals Society of China, 2022, 32: 4088−4098. doi: 10.1016/ S1003-6326(22)66080-1.

[26] JIAO Fen, LI Wei, WANG Xu, YANG Cong-ren, ZHANG Zheng-quan, FU Li-wen, QIN Wen-qing. Application of EDTMPS as a novel calcite depressant in scheelite flotation [J]. International Journal of Mining Science and Technology, 2023, 33: 639−647. doi: 10.1016/ j.ijmst.2022.12.012.

[27] WEI Qian, DONG Liu-yang, YANG Cong-ren, LIU Xue-duan, JIAO Fen, QIN Wen-qing. Selective depression mechanism of combination of lime and sodium humate on arsenopyrite in flotation separation of Zn–As bulk concentrate [J]. Transactions of Nonferrous Metals Society of China, 2022, 32: 668−681. doi: 10.1016/S1003-6326(22)65824-2.

[28] LI Jia-lei, MA Yin-yu, LI Guang-li, LIU Zhi-cheng, NING Shuai, PEI Bin, LANG Zhao-you, LIU Rui-zeng, LIU Dian-wen. Depression mechanism of $ZnSO_4$ and Na_2CO_3 on talc flotation [J]. Transactions of Nonferrous Metals Society of China, 2023, 33: 1559−1571. doi: 10.1016/S1003-6326(23) 66203-X.

[29] JIA Xiao-dong, SONG Kai-wei, CAI Jin-peng, SU Chao, XU Xiao-hui, MA Yin-yu, SHEN Pei-lun, LIU Dian-wen. Effect of oxygen and sodium sulfide on flotation of cuprite and its modification mechanism [J]. Transactions of Nonferrous Metals Society of China, 2023, 33: 1233−1243. doi: 10.1016/S1003-6326(23)66178-3.

[30] ALLAN G F, HEYES G W, ILYAS S, KIM H. Prediction of grade and recovery in flotation from physicochemical and operational aspects using machine learning models [J]. Minerals Engineering, 2022, 183: 107627. doi: 10.1016/ j.mineng.2022.107627.

[31] SUN Hao-ran, YANG Bin, ZHU Zhang-lei, YIN Wan-zhong, SHENG Qiu-yue, HOU Ying, YAO Jin. New insights into selective-depression mechanism of novel depressant EDTMPS on magnesite and quartz surfaces: Adsorption mechanism, DFT calculations, and adsorption model [J]. Minerals Engineering, 2021, 160: 106660. doi: 10.1016/j. mineng.2020.106660.

[32] YAO Jin, SUN Hao-ran, BAN Xiao-qi, YIN Wan-zhong. Analysis of selective modification of sodium dihydrogen phosphate on surfaces of magnesite and dolomite: Reverse flotation separation, adsorption mechanism, and density functional theory calculations [J]. Colloids and Surfaces A: Physicochemical and Engineering Aspects, 2021, 618: 126448. doi: 10.1016/j.colsurfa.2021.126448.

[33] ELMAHDY A M, MIRNEZAMI M, FINCH J A. Zeta potential of air bubbles in presence of frothers [J]. International Journal of Mineral Processing, 2008, 89: 40−43. doi: 10.1016/j.minpro.2008.09.003.

[34] WANG Yu-hua, SUN Ning, CHU Hao-ran, ZHENG Xia-yu, LU Dong-fang, ZHENG Hai-tao. Surface dissolution behavior and its influences on the flotation separation of spodumene from silicates [J]. Separation Science and Technology, 2021, 56: 1407−1417. doi: 10.1080/ 01496395.2020.1768120.

[35] LIMA R M F, BRANDAO P R G, PERES A E C. The infrared spectra of amine collectors used in the flotation of iron ores [J]. Minerals Engineering, 2005, 18: 267−273. doi: 10.1016/j.mineng.2004.10.016.

[36] GAO Zhi-yong, DENG Jian, SUN Wei, WANG Jian-jun, LIU Yun-feng, XU Feng-ping, WANG Qing-hong. Selective flotation of scheelite from calcite using a novel reagent scheme [J]. Mineral Processing and Extractive Metallurgy Review, 2022, 43: 137−149. doi: 10.1080/08827508.2020. 1825956.

[37] QIN Wen-qing, HU Jun-jie, ZHU Hai-ling, JIAO Fen, JIA Wen-hao, HAN Jun-wei, CHEN Chen. Effect of depressants on flotation separation of magnesite from dolomite and calcite [J]. International Journal of Mining Science and Technology, 2023, 33: 83−91. doi: 10.1016/j.ijmst.2022.09. 018.

[38] LU Yi-ping, ZHANG Ming-qiang, FENG Qi-ming, LONG Tao, QU Le-ming, ZHANG Guo-fan. Effect of sodium hexametaphosphate on separation of serpentine from pyrite [J]. Transactions of Nonferrous Metals Society of China, 2011, 21: 208−213. doi: 10.1016/s1003-6326(11)60701-2.

[39] GONG Xiu-feng, YAO Jin, YANG Bin, YIN Wan-zhong, GUO Jun, SONG Ning-bo, WANG Yu-lian, SUN Hao-ran. Activation−inhibition mechanism of diammonium hydrogen phosphate in flotation separation of brucite and calcite [J]. Journal of Environmental Chemical Engineering, 2023, 11: 110184. doi: 10.1016/j.jece.2023.110184.

[40] GONG Xiu-feng, YAO Jin, YANG Bin, YIN Wan-zhong, GUO Jun, SONG Ning-bo, WANG Yu-lian, SUN Hao-ran, FU Ya-feng. Selective activation of new regulator SMP in reverse flotation separation of brucite and calcite [J]. Colloids and Surfaces A: Physicochemical and Engineering Aspects, 2023, 675: 132049. doi: 10.1016/j.colsurfa.2023. 132049.

调整剂磷酸二氢钾强化十二胺体系中水镁石和方解石的浮选分离

宫秀峰[1]，姚 金[1]，杨 斌[2]，印万忠[1]，王余莲[3]，付亚峰[4]

1. 东北大学 资源与土木工程学院，沈阳 110819；
2. 中国矿业大学 化学工程学院，徐州 221163；
3. 沈阳理工大学 材料科学与工程学院，沈阳 110159
4. 鞍钢集团北京研究院有限公司，北京 102200

摘 要：为了实现水镁石和方解石的高效浮选分离，以十二胺(DDA)为捕收剂、磷酸二氢钾(PDP)为调整剂，进行两种矿物的浮选分离实验。通过接触角测量、zeta 电位检测、溶液化学计算、傅里叶红外光谱分析和 X 射线光电子能谱检测等方法，研究 DDA 和 PDP 在两种矿物分选中的作用机理。浮选结果表明，当 DDA 用量为 35 mg/L、PDP 用量为 40 mg/L 时，水镁石与方解石的最大浮游差为 79.81%，选择性分离指数为 6.46。检测分析表明，PDP 的主要溶解组分 HPO_4^{2-}选择性地强烈吸附于方解石表面的 Ca 位点，促进了 DDA 的主要溶解组分 RNH_3^+在方解石表面的吸附，而水镁石基本不受 PDP 的影响。因此，PDP 是 DDA 体系中实现水镁石和方解石反浮选分离的有效调整剂。

关键词：水镁石；方解石；选择性吸附；浮选分离

(Edited by Wei-ping CHEN)